

## Decision-making of alternative pylon shapes of a benchmark cable-stayed bridge using seismic risk assessment

Vahid Akhoondzade-Noghabi\* and Khosrow Bargi<sup>a</sup>

*School of Civil Engineering, College of Engineering, University of Tehran, Tehran, Iran*

*(Received December 15, 2014, Revised September 6, 2016, Accepted September 24, 2016)*

**Abstract.** One of the main applications of seismic risk assessment is that an specific design could be selected for a bridge from different alternatives by considering damage losses alongside primary construction costs. Therefore, in this paper, the focus is on selecting the shape of pylon, which is a changeable component in the design of a cable-stayed bridge, as a double criterion decision-making problem. Different shapes of pylons include H, A, Y, and diamond shape, and the two criterion are construction costs and probable earthquake losses. In this research, decision-making is performed by using developed seismic risk assessment process as a powerful method. Considering the existing uncertainties in seismic risk assessment process, the combined incremental dynamic analysis (IDA) and uniform design (UD) based fragility assessment method is proposed, in which the UD method is utilized to provide the logical capacity models of the structure, and the IDA method is employed to give the probabilistic seismic demand model of structure. Using the aforementioned models and by defining damage states, the fragility curves of the bridge system are obtained for the different pylon shapes usage. Finally, by combining the fragility curves with damage losses and implementing the proposed cost-loss-benefit (CLB) method, the seismic risk assessment process is developed with financial-comparative approach. Thus, the optimal shape of the pylon can be determined using double criterion decision-making. The final results of decision-making study indicate that the optimal pylon shapes for the studied span of cable-stayed bridge are, respectively, H shape, diamond shape, Y shape, and A shape.

**Keywords:** cable-stayed bridge; pylon shape; seismic risk assessment; double criterion decision-making; financial - comparative approach; Cost-Loss-Benefit (CLB) method

### 1. Introduction

There are several reports of damaged bridges in the earthquakes such as 2008 Wenchuan earthquake or 1999 Taiwan Chi-Chi earthquake. It goes without saying that bridges, as one the most important facilities of transportation, must remain serviceable for the purpose of emergency disaster relief. Therefore, in addition to design according to code requirements, methods for the seismic risk assessment of the existing bridges are needed to be presented. Seismic risk assessment could help engineers select an economically justified structural design from various structural

---

\*Corresponding author, Ph.D. Student, E-mail: [akhoondzade@ut.ac.ir](mailto:akhoondzade@ut.ac.ir)

<sup>a</sup>Professor, E-mail: [kbargi@ut.ac.ir](mailto:kbargi@ut.ac.ir)

alternatives by considering damage losses along with primary construction costs. However, this is still not a standard design process. But, the concept of performance based design process is based on the total probability theorem which is made the main structure of risk assessment models (Tesfamariam and Goda 2013).

Cable-stayed bridges are known to be a good option for long spans. Due to their long spans, study of the cable-stayed bridges must consider the nonlinear behavior (Ren and Obata 1999). In Nazmy and Abdel-Ghaffar's study (1990), a model was proposed to take into account the nonlinear behavior due to the sagging of cables. Modeling of the nonlinearity caused by  $p$ - $\Delta$  effect was recommended by (Ren and Obata 1999). The nonlinear behavior of concrete is usually simulated by Mander *et al.* models (1988). Also, the ASTM reinforcement bar model is suggested in Caltrans (2004).

Intense damages to cable-stayed bridges are reported in some cases of earthquakes, such as Chi-Lu bridge in Taiwan during the Chi-Chi earthquake (Chang *et al.* 2004). Their long spans and inherently low damping could be the cause of their vulnerability. Therefore, some of the research implemented over the last few years, has focused on the seismic vulnerability assessment of this type of bridges. In this regard, fragility relationships were presented as a technique for seismic vulnerability assessment of a cable-stayed bridge by Barnawi and Dyke (2014). Vulnerability assessment of a cable-stayed bridge by obtaining fragility curves using structural reliability-based approach is one of the common approaches in research (Casciati *et al.* 2008, Khan and Datta 2010). Yet, the most common approach of calculating the damage probability to obtain the fragility curves, is to use a lognormal distribution function which was implemented by Agrawal *et al.* (2012) for a benchmark cable-stayed bridge. In some cases, to assess seismic performance the combined damage indices are used such as multi-parameter Park - Ang index which was proposed by Wang and Yuan (2009) for a cable-stayed bridge and by Jara *et al.* (2014) for a medium-length span bridge. Also, the suggested index by Li *et al.* (2009) for a cable-stayed bridge has been used to perform seismic risk assessment process. In addition, researchers have proposed different damage states for cable-stayed bridges depending on the studied damage criterion (Li *et al.* 2009, Wang and Yuan 2009, Pang *et al.* 2013).

Seismic risk assessment is usually performed in two steps; vulnerability assessment in the form of fragility curves and loss assessment in the form of total loss ratio estimation (Mander *et al.* 2007). In the vulnerability assessment of bridges, IDA proposed by Vamvatsikos and Cornell (2002) is a common tool to obtain dynamic capacity curves and consequently fragility curves. Mander *et al.* (2007) obtained the fragility curves of bridge piers by assigning Ramberg-Osgood equations to the IDA curves. However, considering the fragility of only one component of the structure yields in an inaccurate estimate of the entire bridge system fragility. Regarding this, the fragility of the entire bridge system is proposed to be calculated by implementing jointly probabilistic model which considers the fragility of components (Nielson and DesRoches 2002).

Owing to the fact that seismic risk assessment requires the combination of fragility curves and damage losses, the use of loss ratio, which is obtained from experimental results is a common approach in the loss assessment (Mander *et al.* 2007, Padgett *et al.* 2010). Calculation of loss ratio is done based on experimental data and calibrating them over the existing bridges (Mander *et al.* 2012).

In order to apply the uncertainty of structure capacity in seismic risk assessment, the Monte-Carlo simulation by Shinozuka *et al.* (2002) and those by Khan and Datta (2010) or the LHS simulation method by Agrawal *et al.* (2012) are generally used. The aforementioned methods have a large number of random samples and, therefore, need to perform a large number of calculations.

In order to reduce the number of the produced random samples, Pang *et al.* (2013) used the UD method to produce the random samples of a bridge, along with the time history method. Different algorithms such as “global optimization” or “threshold accepting” are the basis for producing the random samples in the UD method (Fang *et al.* 2000). On the other hand, because of the uncertainty present in the seismic demand, different methods such as capacity spectrum method (CSM) by Olmos *et al.* (2012) and Jara *et al.* (2013a), time history analysis (THA) by Pang *et al.* (2013) and Yi *et al.* (2007) or IDA by Mander *et al.* (2007) have been usually used. The IDA can be more accurate than the THA, due to step-by-step application of the earthquake. Since, in order to apply the uncertainties of demand and capacity more precisely, in this paper the simultaneous use of IDA method and UD method will be employed.

One of the applications of seismic vulnerability assessment is to compare different design schemes according to their fragility curves in the probabilistic domain. For example, the effect of using lead rubber bearing (LRB) in an extradosed bridge was studied by Kim *et al.* (2008) considering fragility curve fluctuation. In another research, Shinozuka *et al.* (2002) examined the effect of pier steel jacketing by comparing fragility curves of a bridge before and after retrofit. Also, comparison of fragility curves was used by Olmos *et al.* (2012) to study the contribution of some factors such as span length, pier height and piers configuration in the seismic performance of reinforced concrete bridges. For cable-stayed bridge, different connection types between decks and pylons are compared together according to the results of seismic vulnerability assessment by Li *et al.* (2009). Moreover, the effect of different retrofits on fragility curves of cable-stayed bridge was studied by Casciati *et al.* (2008) and Agrawal *et al.* (2012).

In another category of studies in deterministic domain, Domaneschi (2010) and Domaneschi and Martinelli (2012, 2013) were able to compare the effect of different control strategies on a benchmark cable-stayed bridge, by defining two utility functions and six evaluation criterion, respectively. It is notable that all of these functions and criterion were obtained from force and displacement responses, directly. Also, Jara *et al.* (2013b) and Fanfang *et al.* (2014) studied an irregular bridge with LRB and a cable-stayed bridge with viscous fluid damper, to identify the best behavior parameters of mentioned isolation devices.

The research on different pylon shape effect in cable-stayed bridge that has been reported in the literature is limited to the investigation of structural responses such as internal forces or displacements (Bhagwat *et al.* 2009, 2011, Shah *et al.* 2010). As a result, it is obvious that a complete judgment cannot be achieved between different pylon shapes, only through separately comparing the forces and displacements of components in a deterministic domain. However, judging based on the probabilistic loss of the bridge system as consequences of earthquake, is the more effective way to compare different design schemes. Moreover, this must be done as a combination of the earthquake impacts on the all components. Such a judgment which is the purpose of this paper, cannot be achieved unless the complete seismic risk assessment process is performed on a cable-stayed bridge with different pylon shapes. However, the reduction of earthquake losses is not sufficient for the justifiable solution about seismic risk mitigation, and the construction costs also must be taken into account. Therefore, the purpose of this paper is to choose the optimal pylon shape of a cable-stayed bridge as a double criterion decision-making problem. It should be noted that this paper considers a primary design of a structure, not a retrofit scheme. So an “alternative” design is a design that could be implemented instead of the present design of a benchmark cable-stayed bridge.

In the field of decision-making, Mackie and Stojadinovic (2005) by using loss as a decision criteria, explained the effects of design parameters on the seismic. Also, in the form of a multi-

criterion decision-making problem and by applying analytical hierarchy process as a decision making tool, Sasmal *et al.* (2007) were able to prioritize studied bridges for the rehabilitation funds. Also, in order to improve the decision-making space, the use of time-dependent risk indicator along with redundancy indicator was suggested by Deco and Frangopol (2011).

To reach the goal of this paper, an example of a cable-stayed bridge is selected as the benchmark study. All the structural features remain the same, except the pylon which is designed in four different shapes. Then, the nonlinear models for each of cases are dynamically analyzed and the IDA curves are obtained for the structure components. The fragility curves of components can be obtained by assigning the probabilistic seismic demand model to them and monitoring the damage limit states. Then, based on an analytical method, the fragility curve for the bridge system is obtained from the curves of its components. Then the expected annual loss can be found for different pylon shapes by utilizing the loss ratio and hazard-recurrence relationship. Finally, the proper decision is made about the optimal pylon shape by applying the proposed Cost-Loss-Benefit method and defining a hybrid decision criteria. The process of implemented decision-making problem to achieve a justifiable solution about seismic risk mitigation is shown in Fig. 1.

It should be noted that in this study, the UD method and the IDA method are used to consider the uncertainties in demand and capacity, respectively. Also the probabilistic seismic demand distribution is developed using IDA curves. However, in the previous research THA was used to estimate the probabilistic seismic demand distribution (Pang *et al.* 2013), and even when the IDA method was used, the fragility curves were developed just by using the percentile IDA curves (Mander *et al.* 2007).

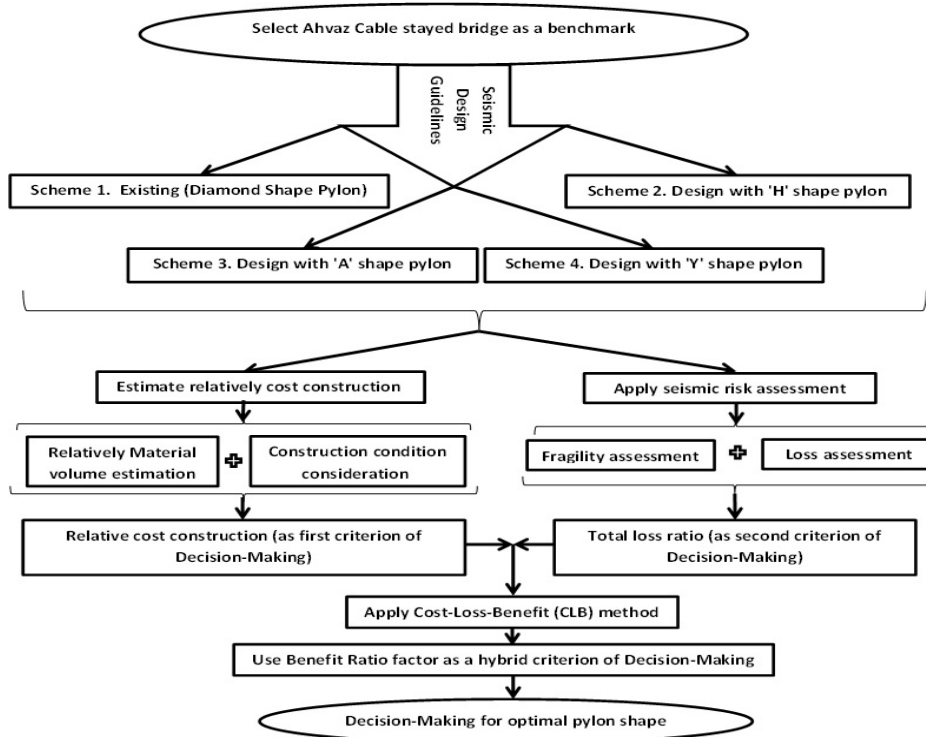
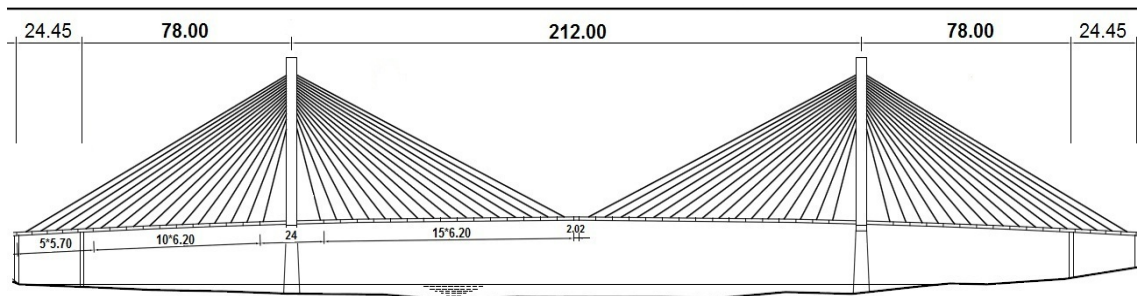


Fig. 1 Solving process for Decision-Making problem of this paper

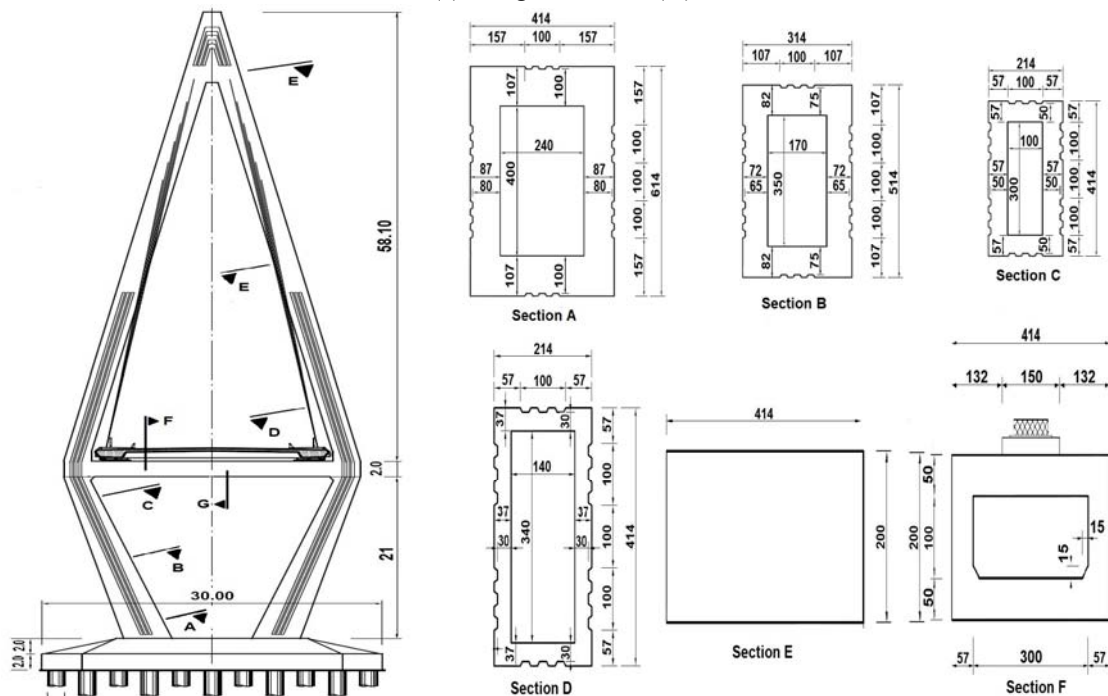
## 2. Description of the benchmark and models with four different design schemes

Since this paper tries to study on a benchmark cable-stayed bridge, first it is necessary to develop the required models with four different pylon shapes. The Ahvaz cable-stayed bridge with diamond pylon shape located in Iran, is selected as the benchmark and shown schematically in Figs. 2(a)-(c).

The Ahvaz cable-stayed bridge has two diamond shape concrete pylons with a mid span of 212 meters. The pylons are 81 meters high and cross-sections are hollow concrete, the dimension and thickness of which change along the height. The cross beam of the pylon is hollow section in the middle and bold section in the sides and is connected to deck by elastomeric bearing pads. The



(a) Bridge side view (m)



(b) Pylon side view (m)

(c) Pylon sections (cm)

Fig. 2 Drawings of the Ahvaz cable-stayed bridge

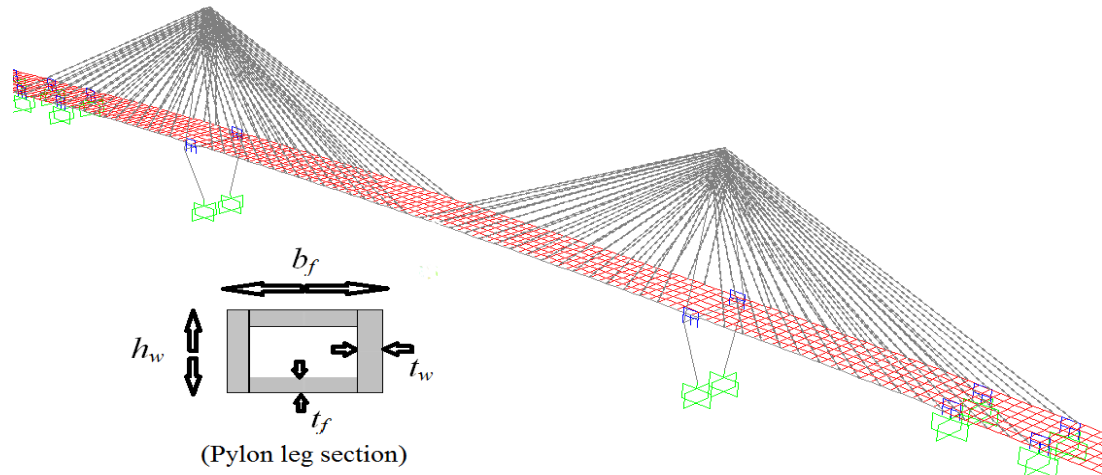


Fig. 3 Model of the cable-stayed bridge developed in SAP2000, and the cross section of pylon leg

composite deck of the bridge includes concrete slabs and steel box girders. The cables have semi fan configuration, and 78 meters side spans are also cables-stayed. The 3D nonlinear model of the bridge is developed based on Caltrans (2004), Aviram *et al.* (2008), SAP2000 recommendations and is illustrated in Fig. 3.

It is notable that utilization of SAP2000 software to model and perform dynamic analysis of bridge, can be seen in several research such as Jara *et al.* (2013b, 2014) in the field of seismic performance assessment of bridges, and, Chang *et al.* (2004), Calvi *et al.* (2010), Shah *et al.* (2010) for seismic performance assessment of cable-stayed bridge, or Shinozuko *et al.* (2002), Yi *et al.* (2007), Deco and Frangopol (2011), Agrawal *et al.* (2012), Olmos *et al.* (2012), Jara *et al.* (2013a) in the field of seismic fragility assessment of bridges.

The materials of the developed model including confined and unconfined concrete and reinforcement bars, are defined by (Core model) Mander (1988), (Cover model) Mander (1988) and (ASTM model) Caltrans (2004), respectively. These models can be found in Caltrans section properties in SAP2000. Considering the nonlinear effects due to sagging and neglecting the transversal dynamics of cables, the cables are modeled using single truss element with equivalent elastic modulus (Domaneschi and Martinelli 2013) based on the Eq. (1) (Ren and Obata 1999, Raheem and Hayashikawa 2013)

$$E_{eq} = \frac{E}{1 + \frac{(L_0 \gamma)^2 (\sigma_1 + \sigma_2)}{24 \sigma_1^2 \sigma_2^2} E} \quad (1)$$

Where  $E_{eq}$  is the equivalent elastic modulus of the cable,  $E$  is the elastic modulus of the cable material,  $L_0$  is the length of the horizontal projection of the cable,  $\sigma_1$  and  $\sigma_2$  and are tension stresses of the cable in the beginning and at the end of a certain loading process.

Considering the nonlinear behavior and axial force-bending moment interactions, the pylons are simulated by assigning distributed plasticity fiber model to the section of nonlinear beam-column element (Nazmy and Abdel-Ghaffar 1990, Aviram *et al.* 2008). Due to the large geometric dimensions of the structure, the nonlinear effect of P- $\Delta$  is considered. In order to consider the

nonlinear behavior of the cross beam in the pylon, a rotational plastic hinge is added to its both endpoints. The concept of hinge definition and parameters provided based on (Aviram *et al.* 2008)'s recommendations. The behavior of piers in side spans is modeled using nonlinear link element. The elastomeric bearing pads are modeled by link elements with bilinear plastic model provided by Makris and Zhang (2002). The concrete slab of deck is modeled by shell elements supported by a plane frame of steel girders (Domaneschi and Martinelli 2013). It is notable that since the girders must remain elastic, they are modeled using elastic steel beam-column element. Considering the cable configuration, damping of the structure is assumed to be 3% (Tang 1992, Kawashima *et al.* 1993).

Besides the existing diamond shape of the pylon, the benchmark bridge is designed with three other pylon shapes including A, Y, and H shape. The design is performed using guidelines provided by Tang (1992) and conceptual seismic design of cable-stayed bridge proposed by Calvi *et al.* (2010). diamond, A, and H shape are common pylon shapes for two planes cable configurations in cable-stayed bridges (Svensson 2013) and Y shape is used by researchers in Shah *et al.* (2010). The pylon shapes are illustrated schematically in Fig. 4.

The results show that designing the bridge with different pylon shapes, causes changes in design forces and consequently in dimensions of the three main substructures including pylon, deck and cables. Also, the design parameters of the other components such as bearing devices and cable anchorage are changed in different design schemes. After the design process, the volume of used material for four different design schemes can be presented relatively. If the material usage for the benchmark bridge (with diamond pylon shape) is stated by the value "1", then the material used for other three cases is given relatively for different substructures in Table 1. Besides, the

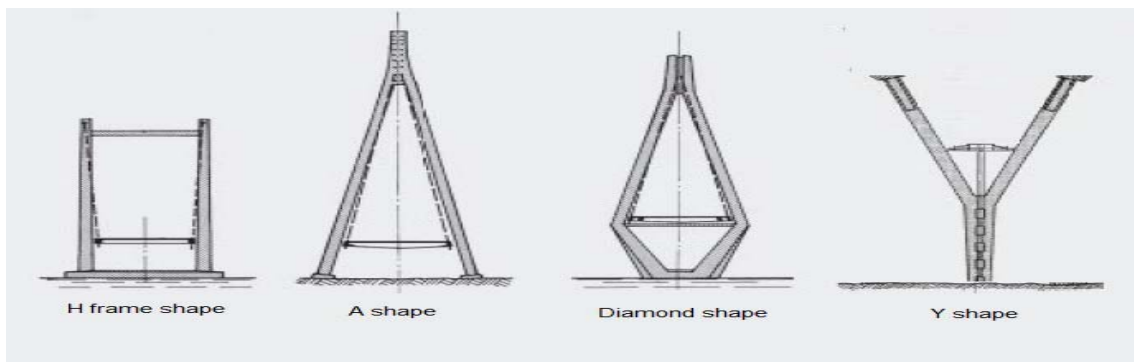


Fig. 4 Different pylon shapes (Svensson 2013 and Shah *et al.* 2010)

Table 1 Material volume coefficients of four designed Schemes

Pylon Shape	Material Volume Coefficient of				Bridge system
	Substructures				
	Pylons	Deck	Cables	Others	
Diamond shape	1(23%)	1(40%)	1(18%)	1(19%)	1
H shape	0.98(20%)	1.04(42%)	1.05(20%)	1(18%)	1.06
Y shape	1.39(24%)	1.03(41%)	1.08(21%)	1(16%)	1.22
A shape	1.25(22%)	1.02(40%)	1.11(22%)	1(16%)	1.13

values in parentheses show the contribution percentage of the substructures in the total cost of the bridge. Constitutive material of Pylon: concrete and steel rebar, Deck: concrete slab and steel girders, Cable: steel strand, Others: cable anchorage and bearing devices

As mentioned before, all four schemes are designed by considering code-based methods which are generally quick and methods for engineers to use. These methods are usually based on force and displacement and do not consider the damage and loss issues specifically. Hence, we need a more precise tool such as seismic risk assessment to study the structure performance more accurately which is applied in the following to all 4 design schemes.

### 3. Seismic risk assessment process

After modeling the four different bridges, the seismic risk assessment process must be separately performed on each of them. This process will be conducted in two steps including seismic fragility assessment and total loss ratio estimation. Developing the fragility curve is done using IDA method (Vamvatsikos and Cornell 2002) and probabilistic seismic demand model (PSDM) estimation of the structure. The PSDM of the bridge is obtained by assigning the double parameter lognormal distribution to the IDA curves (Mander *et al.* 2007, Tesfamariam and Goda 2013). Different damage states of the structure can be defined by assigning double parameter lognormal probabilistic distribution to the capacity criteria of the structure (Mander *et al.* 2007, Casciati *et al.* 2008, Tesfamariam and Goda 2013). Also, a combined method is used to consider the uncertainties of demand and capacity of the structure to seismic fragility assessment, more accurately. This method needs the following steps to simultaneously use UD and IDA methods to apply uncertainties of capacity and demand, respectively.

#### 3.1 IDA and UD-based seismic fragility assessment procedure

##### Step 1 - Choosing the input earthquake records

Normally, 10 to 20 earthquake records are used for PSDM estimation (Vamvatsikos and Cornell 2002). Therefore, 15 records are provided for this research through Pacific earthquake engineering research center (PEER) strong ground motion Database (<http://peer.berkeley.edu/smcat>) which are modified based on uniform hazard spectrum (UHS) approach (Casciati *et al.* 2008, Tesfamariam and Goda 2013). This is done by matching the average spectrum of the records with that of the UHS. Considering the seismic characteristics of the region, all the records are selected for moment magnitudes 6.3 to 7 and 20 to 80 Km distance between source and site. The record spectra are plotted by Seismomatch (Seismosoft-2013) and are illustrated in Fig. 5.

##### Step 2 - Defining the random capacity parameters of the structure

The parameters which are effective on the structure capacity are material behavior and geometric parameters. The first group of parameters deals with fiber hinges and nonlinear behavior of material and the second group deals with pylon cross-sections of the cable-stayed bridge (shown in Fig. 3). Besides the exact values for each of these parameters as a mean value, an upper bound and a lower bound are also defined. For the Ahvaz cable-stayed bridge, these parameters are presented as random variables along with their probabilistic distributions in Table 2.

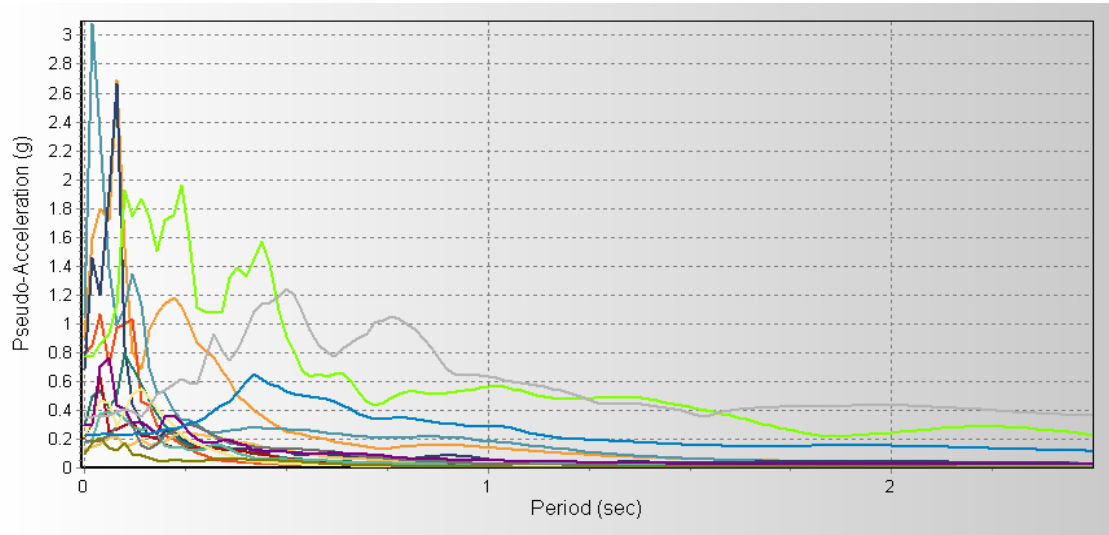


Fig. 5 Acceleration spectrum for the selected records

Table 2 effective parameters on the structure capacity as random variables

Random variable	Distribution	Mean	Lower limit	Upper Limit
$f_y$	Lognormal	400 Mpa	320	480
$f'_c$ (cover)	Lognormal	30 Mpa	23	37
$\varepsilon_c$ (cover)	Lognormal	0.002	0.0012	0.0028
$\varepsilon_{cu}$ (cover)	Lognormal	0.006	0.0036	0.0084
$f'_c$ (core)	Lognormal	35 Mpa	25	45
$f'_{cu}$ (core)	Lognormal	25 Mpa	20	30
$\varepsilon_c$ (core)	Lognormal	0.004	0.0024	0.0056
$\varepsilon_{cu}$ (core)	Lognormal	0.015	0.0065	0.025
E	Lognormal	200000 Mpa	180000	220000
$\alpha$	Lognormal	0.0012	0.0007	0.0017
$t$ (cover)	Normal	0.05 m	0.04	0.06
$b_f$	Normal	6 m	5.5	6.5
$t_f$	Normal	0.8 m	0.6	1
$h_w$	Normal	4 m	3.65	4.35
$t_w$	Normal	1 m	0.8	1.2

$f_y$ : yielding stress of steel, E: Elasticity modulus of steel,  $\alpha$ : post yield to initial stiffness ratio of steel,  $f'_c$ ,  $f'_{cu}$ ,  $\varepsilon_c$  and  $\varepsilon_{cu}$ : stress-strain parameters of concrete behavior,  $t$ (cover),  $b_f$ ,  $t_f$ ,  $h_w$ ,  $t_w$ : geometric parameters (shown in Fig. 3)

Assigning random values to the effective parameters and generating the bridge models to perform the analysis are done using the UD method. So structure samples are provided based on the UD

table which is produced by threshold accepting algorithm as a refined local search algorithm (Fang *et al.* 2000). The UD table is entitled as  $Un(L_f)$ , where 'n' is the number of required tests, 'f' represents the number of effective parameters, and 'L' indicates the number of states for each factor. In this study, the number of tests (number of rows in UD table) is equal to the number of records which are selected in step 1 and each one of the records is assigned to each row of the table. According to Table 2 the number of parameters is 15. To facilitate the creation of UD table, the number of states for each parameter is assumed to be 15. Considering the number of states for each parameter, the value of each effective parameter on the capacity is divided into 15 values between its lower and upper limits. Thus a value can be defined for each parameter as the incremental step. Based on mentioned assumptions and the threshold accepting algorithm, the values of UD table are generated as shown in Table 3 in which the produced numbers are the criteria for generating the random capacity parameters of the structure.

Each row of the table results in a randomly characterized structure to be analyzed for the corresponding record which is assigned to the row. If 'k' is the number in i'th row and j'th column, this means that the j'th factor of the effective parameters will take the value of lower bound plus k times the incremental step. The values of the other effective parameters can be determined in such way. Finally, for each row of the table, a sample of the bridge is developed with certain but random capacity parameters to analyze under the corresponding record.

### Step 3 - Determining the Probabilistic Seismic Demand Model (PSDM)

In this step, first the developed models are analyzed under the dead load, and then the earthquake records are applied to the deformed model. Each record selected in Fig. 5 is divided to 15 different scales, relatively and based on its PGA (Vamvatsikos and Cornell 2002). After the

Table3 Random values of UD table

Test	Factor														
	1	2	3	4	5	6	7	8	9	10	11	12	13	14	15
1	12	14	1	9	11	11	2	8	2	7	9	10	15	13	10
2	13	1	8	10	3	1	8	5	7	2	5	14	10	12	5
3	7	3	2	8	5	13	1	13	4	14	10	6	9	5	11
4	4	4	15	13	10	14	4	14	3	5	14	9	7	9	9
5	15	9	10	4	6	5	3	4	5	9	11	5	12	15	13
6	8	1	11	7	14	12	11	1	6	3	2	4	13	8	12
7	1	6	9	6	15	2	5	12	12	13	13	1	3	3	13
8	9	10	3	14	13	3	6	15	13	6	8	7	14	4	15
9	11	2	7	15	9	4	15	3	11	12	7	15	2	7	2
10	14	8	5	1	12	9	11	6	8	5	15	2	8	10	14
11	10	13	12	2	1	7	7	7	15	11	3	6	11	2	3
12	5	5	6	12	2	6	12	9	14	8	4	11	4	1	1
13	2	7	14	3	4	15	14	11	9	10	6	8	5	6	4
14	6	15	4	11	7	8	9	10	10	15	7	12	1	11	6
15	3	11	13	6	8	10	10	2	1	1	1	13	6	14	7

first stage of the analysis, each scaled record is applied to the aforementioned nonlinear models using time history (direct integration method) in SAP2000 v15. Then four seismic demands of the structure are monitored: pylon head displacement, critical pylon section curvature, cable tension, and bearing displacement. It is notable that the shape of pylon has no significant effect on bending stress in deck (Bhagwat *et al.* 2009, 2011), so in this paper it is not monitored.

Since failure probability of cable-stayed bridge is not very sensitive to the variation of angle of ground motion excitation (Khan *et al.* 2006), in this paper each records is applied separately in longitudinal and transverse directions. Yet, the analysis results of this paper indicate that the pylon shape has more effect on the bearing displacement under longitudinal excitations, so the fragility assessment for this response is done for longitudinal excitations. However, the other three demands are monitored for critical response between longitudinal and transverse excitations. The maximum values of quadruple responses are obtained for each scale in front of their PGA, and thus one point of the IDA curve is determined. Considering the fact that cable-stayed bridges have long periods, spectral pseudo acceleration of the fundamental period ( $S_a(T_1)$ ) will be used as intensity measure instead of PGA that is a high frequency measure. For this purpose,  $S_a(T_1)$  is determined for each existing record according to the spectra of Fig. 5, and IDA curves are plotted correspondingly. This process is done for all scales and records. Thus, 15 IDA curves are developed for each of four schemes. These curves are illustrated in Figs. 6(a)-(d) for the benchmark bridge with Diamond pylon shape, and for the four monitored responses.

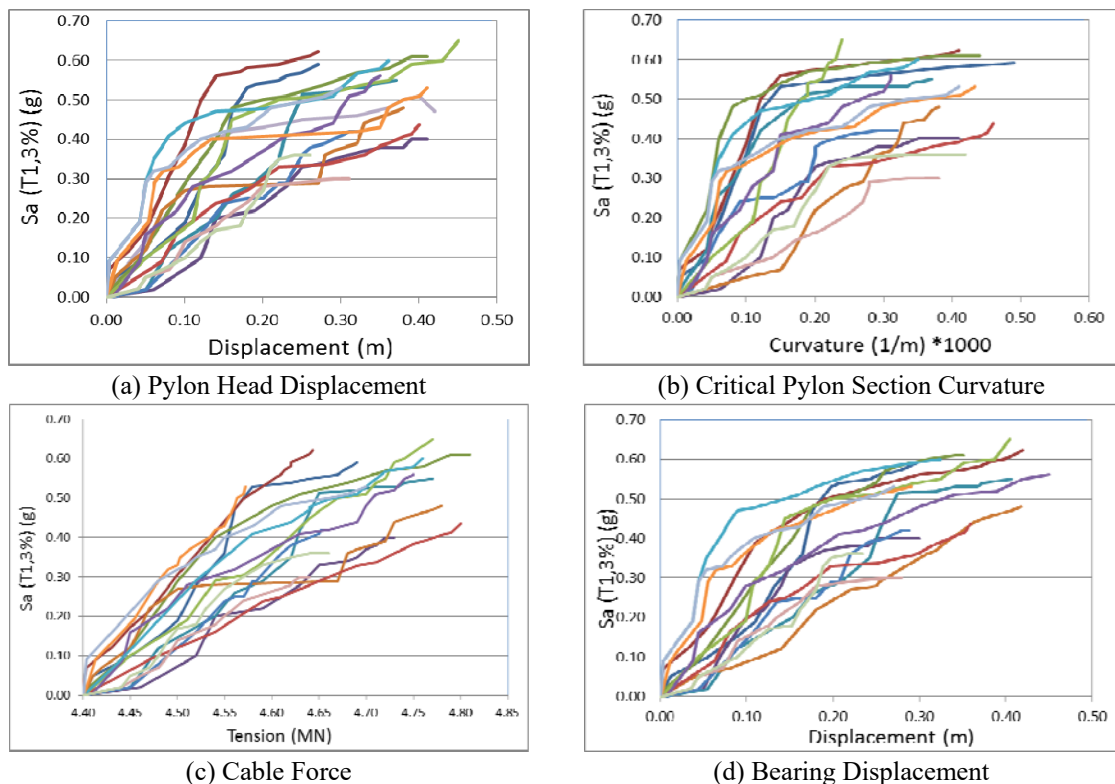


Fig. 6 IDA curves of the benchmark (each color of the curves relates to an specific record)

For the PSDM of a highway bridge, Mander *et al.* (2007) showed that the Ramberg-Osgood relationship could be a proper estimation of the mean lognormal distribution

$$EDP = \frac{IM}{k} \left( 1 + \left( \frac{IM}{IM_c} \right)^{r-1} \right) \quad (2)$$

Where  $EDP$  is the engineering demand parameter which consists of the seismic responses of the structure,  $k$  is the initial stiffness of the IDA curve,  $IM_c$  is a value of the intensity measure which causes the structure to collapse, and  $r$  is the Ramberg-Osgood relationship constant.

It should be noted that by using  $S_a(T_1)$  as an intensity measure, the IM-EDP relationship has less variability and dispersion than using PGA (Jara *et al.* 2014). Also, by assigning the Ramberg-Osgood relationship as the mean lognormal distribution of the IDA curves of the cable-stayed bridge, it is observed that the “ $r$ ” parameter has a small deviation in different points of curve. Thus, by allocating a reasonable value to  $r$ , the values of parameters  $k$  and  $IM_c$  and their corresponding standard deviations can be calculated by least square method. The standard deviation for this distribution is defined by the Eq. (3) as a combination of  $\beta_{\ln k}$  and  $\beta_{\ln IM_c}$  standard deviations

$$\beta_{\ln D} = \sqrt{\beta_{\ln k}^2 + \beta_{\ln IM_c}^2} \quad (3)$$

Where  $\beta_{\ln k}$  and  $\beta_{\ln IM_c}$  are standard deviations of lognormal distributions assigned to parameters  $k$  and  $IM_c$  of the Ramberg-Osgood relationship, respectively. And  $\beta_{\ln D}$  is the standard deviation of lognormal distribution assigned to PSDM. Values of mentioned parameters are shown in Table 4.

It is notable that the demand calculated in the end of the step 3, simultaneously considers the uncertainties of the demand and capacity of the structure, because the IDA curves are related to a random record and capacity model. Finally, instead of the IDA curves for each response, a PSDM consisting of mean curve and standard deviation for the benchmark is presented in Figs. 7(a)-(d).

Step 3 is done similarly for other three design schemes which are produced in section 2, and PSDMs are also developed for them.

#### Step 4 - Defining the damage criteria for cable-stayed bridge

Bridge damages are classified in 4 states; slight, moderate, extensive and collapse(failure) (Mander *et al.* 2007, Mander *et al.* 2012, Jara *et al.* 2013a, and Pang *et al.* 2013). It is necessary to

Table 4 Parameters of the Ramberg-Osgood relationship and its standard deviations

Demand parameter	logN distribution parameter	$IM_c$	k	r
Ln(pylon curvature)	mean	0.54	25.12	5.5
	Log-dispersion	0.52	0.44	---
Ln(pylon Disp)	mean	.48	23.8	8.5
	Log-dispersion	0.42	0.39	---
Ln(Bearing Disp)	mean	0.43	20.19	6.4
	Log-dispersion	0.3	0.51	---
Ln(Cable Tension)	mean	>0.65	12	3.1
	Log-dispersion	0.5(assumed)	0.42	---

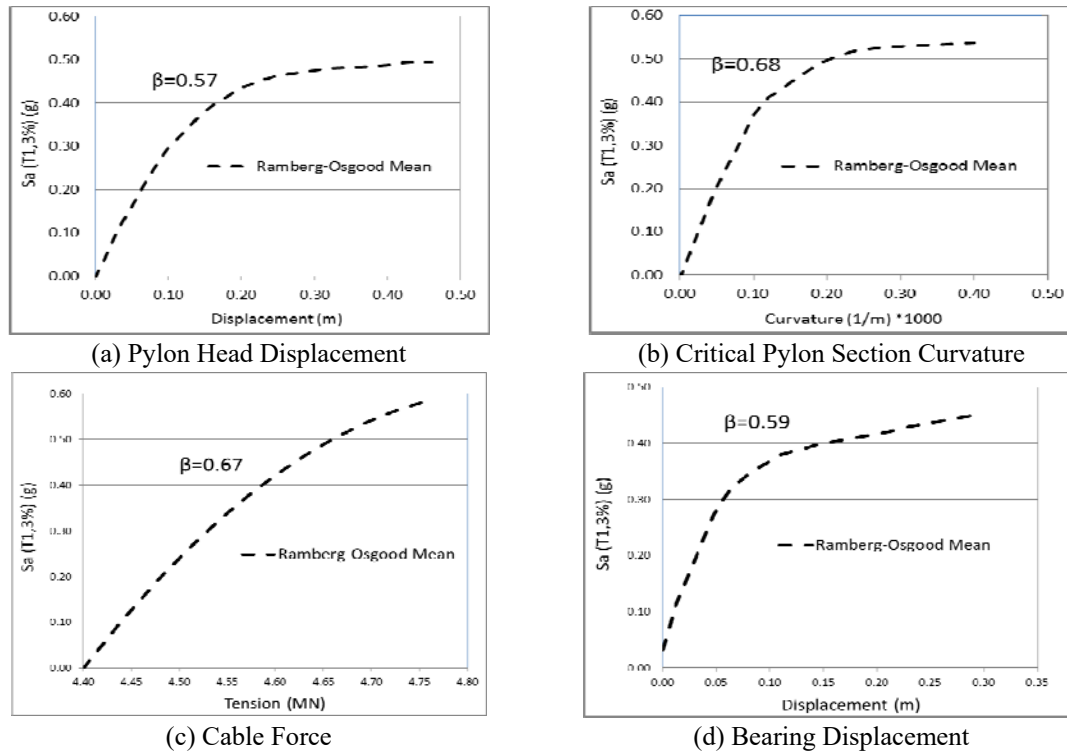


Fig. 7 Probabilistic seismic demand model of the benchmark bridge (with diamond pylon shape)

Table 5 Damage limit states

Capacity Criteria		Lognormal Distribution of Damage Limit States							
Component	Damage index	Slight		Moderate		Extensive		Collapse	
		M*	SD**	M*	SD**	M*	SD**	M*	SD**
Pylon	Curvature Ductility	1.5	0.2	3	0.2	5.5	0.2	7.5	0.2
Pylon Head	Drift	0.011	0.2	0.02	0.2	0.038	0.2	0.06	0.2
Bearing	Displacement (mm)	25	0.2	50	0.2	125	0.2	175	0.2
Cable	Tension(kN)	5500	0.11	6900	0.11	1100	0.11	1350	0.11

\* M: Mean, \*\* SD: Standard Deviation

define each of these damage states by using capacity criteria in order to control the monitored responses when exceeding the damage states. The criteria controlling the seismic responses of a cable-stayed bridge in each damage state is presented as a two parameter lognormal distribution by Pang *et al.* (2013). These criteria which are considered as damage limit states are presented in Table 5.

### Step 5 - Estimation of fragility curves

Fragility curves indicate the probability of exceeding a damage state for different values of intensity measure of the earthquake (Mander *et al.* 2007). The fragility of a component for damage

state ‘ $i$ ’ is defined based on

$$P_f = P[D \geq Cc_i | IM] \quad (4)$$

Where  $P_f$  is the probability of exceedance of damage state  $i$ ,  $D$  is the seismic demand of the structure,  $Cc_i$  is the capacity criterion of the structure in damage state  $i$  which is obtained from Table 5, and  $IM$  is the intensity measure of the earthquake.

Considering the lognormal distributions assigned to the seismic demand and damage criterion of the structure, the probability of exceeding the damage state  $i$  is calculated based on the well-known first-order reliability formula

$$P_f = \phi\left[\frac{\ln\left(\frac{\mu_D}{\mu_{Cc}}\right)}{\sqrt{\beta_{\ln D}^2 + \beta_{\ln Cc}^2}}\right] \quad (5)$$

In which if  $P_f$  is the probability of exceedance of damage state  $i$ , then  $\mu_D$  and  $\beta_{\ln D}$  are the mean and standard deviation of the PSDM, respectively, and  $\mu_{Cc}$  and  $\beta_{\ln Cc}$  are the mean and standard deviation of capacity criteria in damage state  $i$ , respectively.

Eq. (5) develops the fragility curves of the components in four slight, moderate, extensive and collapse damage states. Then, this definition can be used to calculate the fragility of the entire bridge system: “if a component exceeds a certain damage state, it means that the entire bridge experiences the state”.

Considering this definition, the fragility curve for the bridge system can be obtained by using probabilistic principle of “probability union” (Eq. (6)) provided by Ross (2009)

$$P_f[bridge_{system}] = \bigcup_{j=1}^n P_f[component_j] \quad (6)$$

Where  $P_f[bridge_{system}]$  is the probability of the entire bridge system when exceeding the damage state  $i$ ,  $P_f[component_j]$  is the probability of the  $j$ 'th component (monitored response) when exceeding the damage state  $i$ ,  $n$  is the number of effective components on the behavior of the bridge, and  $\cup$  is the probability union function.

In Eq. (6), damage probability of the components is a marginal probabilistic distribution, and damage probability of the bridge system is a jointly probabilistic distribution (Nielson and DesRoches 2007, Ross 2009). The transformation of the marginal distributions to jointly distributions is done based on the multivariable normal distribution theorem, using a matrix the elements of which are determined by the covariance value between each two monitored demands (Ferguson 1967, Ross 2009). However, the lognormal distributions must be transformed into normal distributions, in advance. The correlation coefficients for each pair of the responses given in Table 6 which are calculated by step-by-step control of the monitored responses.

The probability of each component when exceeding a damage state for different values of intensity measure of the earthquake is obtained using Eq. (5), and criterion of the Table 5, and PSDMs of the Fig. 7. The damage probability of the cable-stayed bridge system is calculated based on Eq. (6) using correlation coefficients of Table 6.

This fragility assessment process is also done for other cable-stayed bridges with different pylon shapes designed in section 2. So, the fragility curves of the bridge system and its components for different damage states, alongside different pylon shapes used in the cable stayed-

bridge can be obtained. The mentioned fragility curves of the components are illustrated in Figs. 8-11 and the fragility curve of the entire bridge system is presented in Fig. 12.

Table 6 The correlation coefficient between natural logarithms of the benchmark bridge responses

Parameter	ln(Pylon Curvature)	ln(Pylon Disp*)	ln(Bearing Disp*)	ln(Cable Tension)
ln(Pylon Curvature)	1	0.87	0.71	0.64
ln(Pylon Disp*)	0.87	1	0.76	0.82
ln(Bearing Disp*)	0.71	0.76	1	0.62
ln(Cable Tension)	0.64	0.82	0.62	1

\*Disp: Displacement

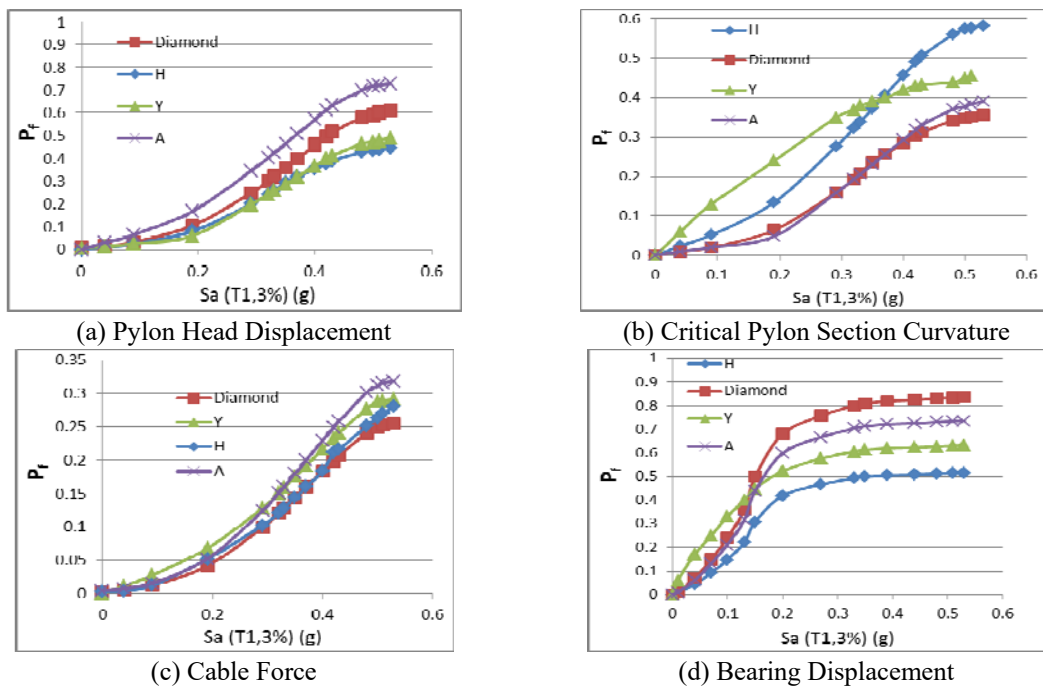


Fig. 8 Fragility Curves for Slight Damage State

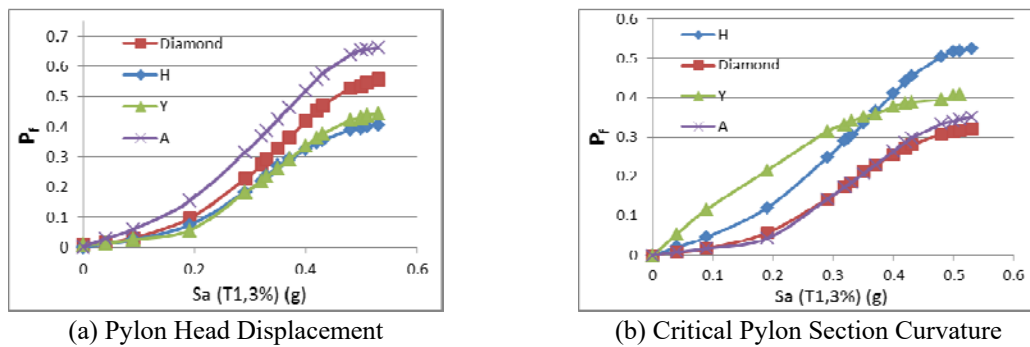


Fig. 9 Fragility Curves for Moderate Damage State

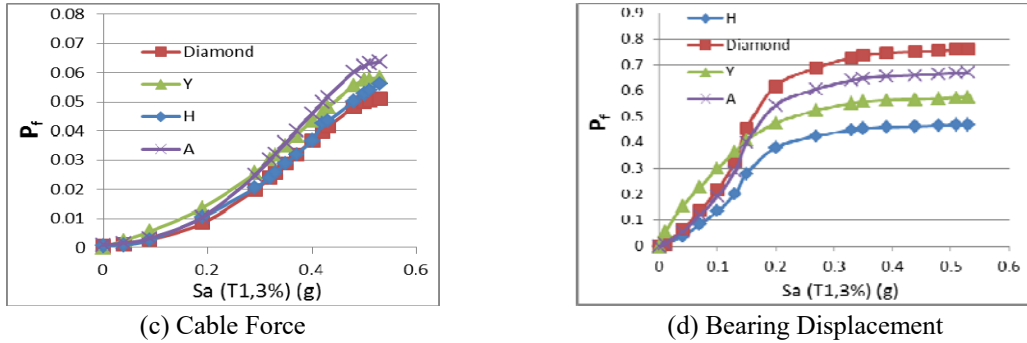


Fig. 9 Continued

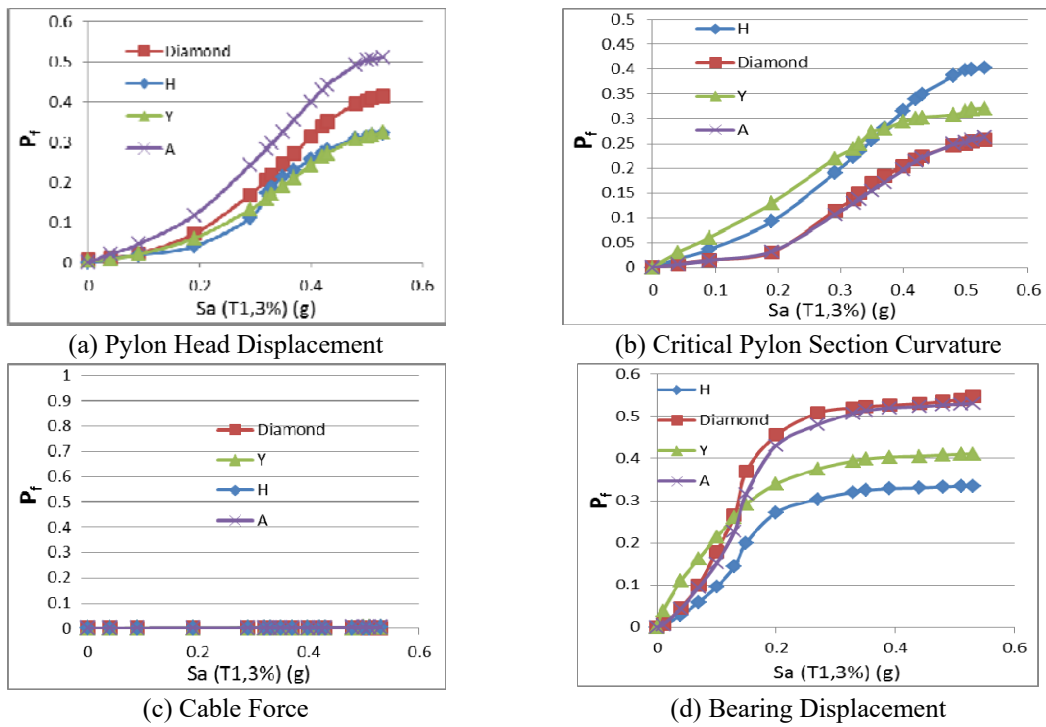


Fig. 10 Fragility Curves for Extensive Damage State

Figs. 8-11 indicate that except for H shape of pylon, bearing device is the most fragile component of the studied bridge. This seems logical considering relatively mediocre seismic resistance of elastomeric bearing pads. Also, the least fragile components are cables which are mainly involved in gravity load carrying and will never experience the collapse state.

It is notable that in some cases it is observed that only the bearing device is in collapse state and other demands are still in the slight damage state; but based on the Eq. (6), it is concluded that the bridge system experiences the collapse state. This does not mean that the bridge is literally collapsed. Indeed, the collapse state for a bridge can indicate that the bridge is no longer operational, because even if one component collapses, the bridge needs to be repaired to maintain

the traffic safety and must be out of service for a while.

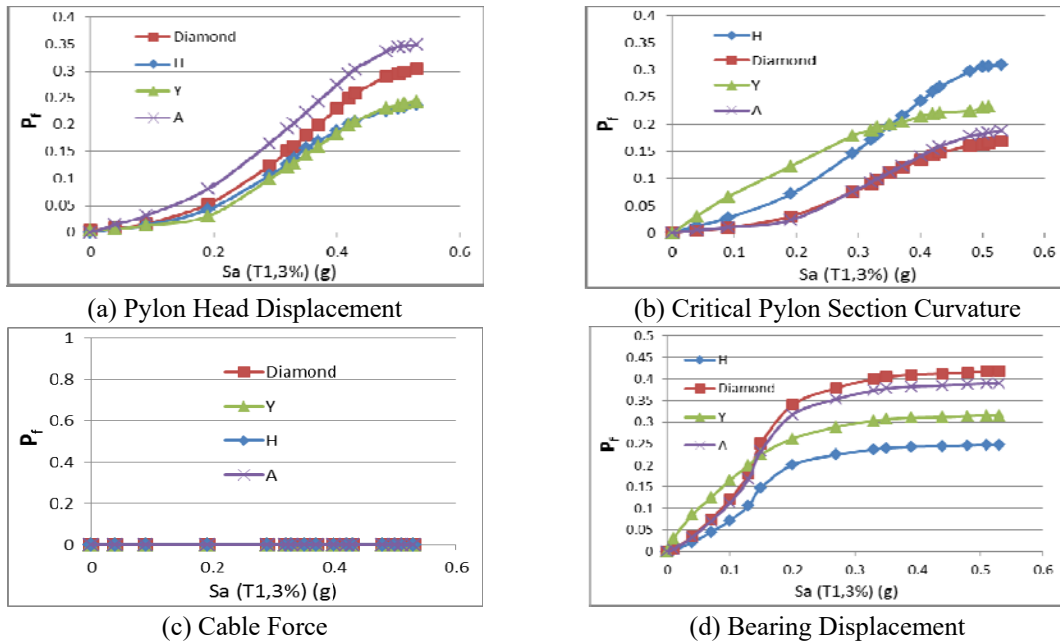


Fig. 11 Fragility Curves for Collapse Damage State

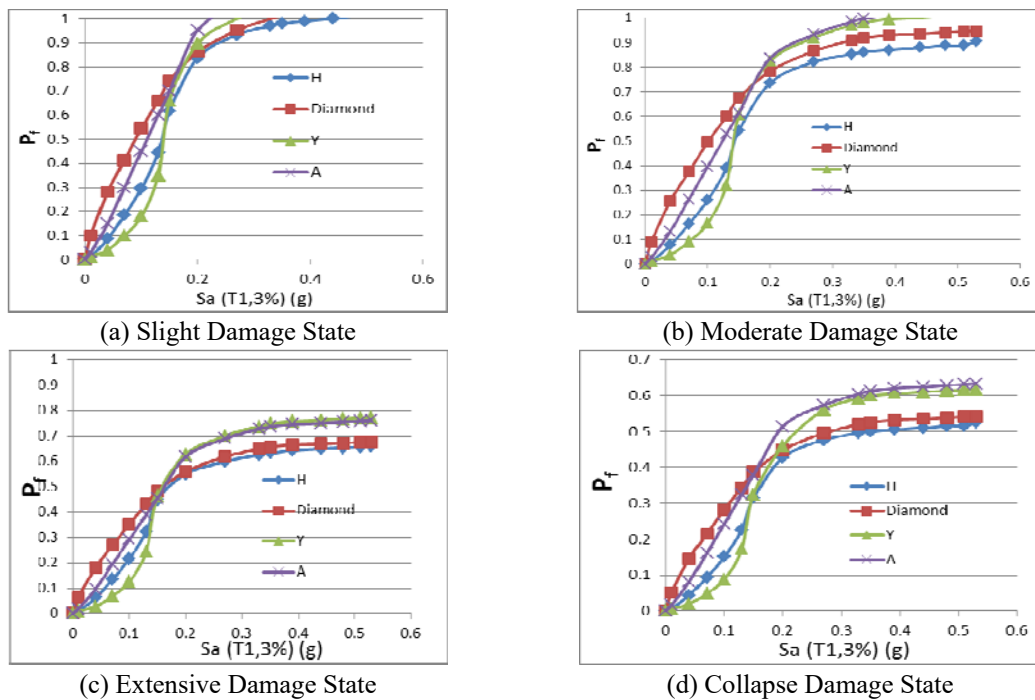


Fig. 12 Fragility Curves of Cable-stayed bridge System with different pylon shapes

The results indicate that the pylon shape has different effects on the fragility level of different components. The probability of pylon head displacement when exceeding a damage state for A shape pylon is higher than the other shapes. This was not unexpected considering the low stiffness of A shape pylon lateral earthquakes, probably (Svensson 2013). The damage probability of pylon curvature is the lowest for diamond shape pylon, and is the highest for H and Y shape. This is probably because of the fact that the diamond shape experiences less moment and therefore less moment curvature due to its divergent legs (Farquhar 2008, Svensson 2013), While H and Y shape have the exact opposite situation due to their vertical legs.

Slight damage state shows that cables are more fragile in A shape pylon than in other three cases. Because A shape of pylon generally has a tension-compression behavior during earthquakes (Svensson 2013), some of the tension will be transferred to cables. Besides, generally, cable tension and pylon head displacement are directly related (Svensson 2013), which can be seen in exceedance probability of these two damage indices in this study.

As mentioned earlier, elastomeric bearing pad displacement is monitored in longitudinal direction. This damage index has the lowest exceedance probability for H shape pylon and the highest for diamond shape. This could be because of the adequate strength of H shape pylon in longitudinal earthquakes due to its portal frame, which causes the elastomeric bearing pads to experience a slight seismic force. However, in the other pylon shapes such as diamond, bearing pads receive large portion of longitudinal earthquake forces. Meanwhile, because the Y shape pylon is a single-legged, all the corresponding damage indices have relatively higher exceedance probability.

Although the fragility of the bridge system differs for different damage states and  $S_a(T_1)$  values, it can be said that generally the damage probability descends in this order: A, Y, diamond, and H shape. The reason that H shape has the best performance is that it has the least damage probability for bearing displacement as the most fragile index, and performs relatively well for other indices. Expressing in more detail, damage index of the bridge system is a weighted sum of damage indices of the components, where the weight of each index is relative to its fragility. In other words, the index with higher fragility probability has more effect on the fragility of the bridge system.

### 3.2 Estimating the total loss ratio curve

Total loss ratio is calculated for different values of intensity measure ( $S_a(T_1)$ ) considering the fragility curves of the entire bridge system and loss ratio of each damage state. This is done using Eq. (7) which is based on the numerical integration of the obtained points of the fragility curve

$$Total\ Loss\ Ratio(IM = im) = \sum_{i=1}^4 [P(DS_i | im) - P(DS_{i+1} | im)] \times LR_i \quad (7)$$

Where  $DS_i$  is the  $i$ 'th damage state, and  $LR_i$  is the loss ratio in  $i$ 'th damage state.

Loss ratio in each damage state is defined as the repair costs to replacement cost ratio (Mander *et al.* (2007), Mander *et al.* (2012), Padgett *et al.* (2010)). In this paper, according to Mander *et al.* (2007), and Padgett *et al.* (2010) suggestions, loss ratio for the bridges is considered as Table 7.

Total loss ratio for any value of earthquake intensity measure calculated by Eq. (7), and is generally reported versus the annual frequency of that intensity measure (Mander *et al.* 2007 and Mander *et al.* 2012). However, by using PDF interpolation technique in fragility assessment step, Yi *et al.* (2007) found the fragility curves based on earthquake return period which is related

Table 7 Loss ratio for the studied bridge in the damage states

Damage state	Slight	Moderate	Extensive	Collapse
Loss ratio(%)	3	8	25	100

directly to its annual frequency. To obtain the annual frequency of intensity measure, it is necessary to estimate the hazard curve of the studied bridge region by an approximate equation. This curve estimates the annual frequency of the occurrence of the earthquake intensity measure. Eq. (8) shows the relationship between the intensity measure of the earthquake and its annual frequency

$$f_a = a(IM)^{-b} \tag{8}$$

Where  $IM$  is the intensity measure of the earthquake,  $f_a$  is the annual frequency and  $a$  and  $b$  are constants of the equation which are obtained by seismological studies of the region.

Parameter  $b$  in Eq. (8) represents the annual hazard-recurrence rate curve of the studied region. According to seismological studies of Iran performed by Gholipour *et al.* (2008) and by assigning the Eq. (8) to the results of the studies, the value for parameter  $b$  is 3.3. The mentioned curve is illustrated in Fig. 13 in a Log-Log space.

Note that the Eq. (8) is presented for PGA parameter. While the results of this paper as mentioned before, are obtained based on  $S_a(T_1)$  as the intensity measure of the earthquake. Transformation of PGA into the corresponding  $S_a(T_1)$  is done by the spectra of the Fig. 5.

The total loss ratio versus its annual frequency of occurrence is calculated for the four different pylon shapes, using Eqs. (7)-(8), and is illustrated in Fig. 14.

The vertical axis in Fig. 14 represents the ratio of probable loss to cost of the bridge, and the horizontal axis represents the annual frequency of the occurrence of that loss state. This frequency is in fact the frequency of the occurrence of an earthquake which causes the mentioned loss state. According to Fig. 14, H and Diamond shape pylons lead to the lower total loss ratios. However, comparing the previous pylon shapes in two different points of the curve might show different results. So a more accurate judgment is required for absolute decision-making of optimal pylon

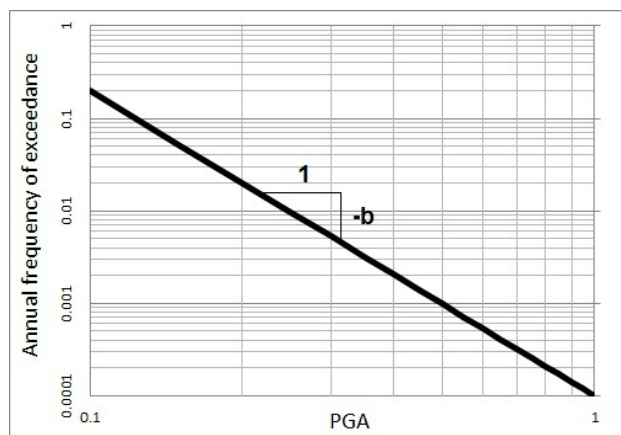


Fig. 13 Hazard curve

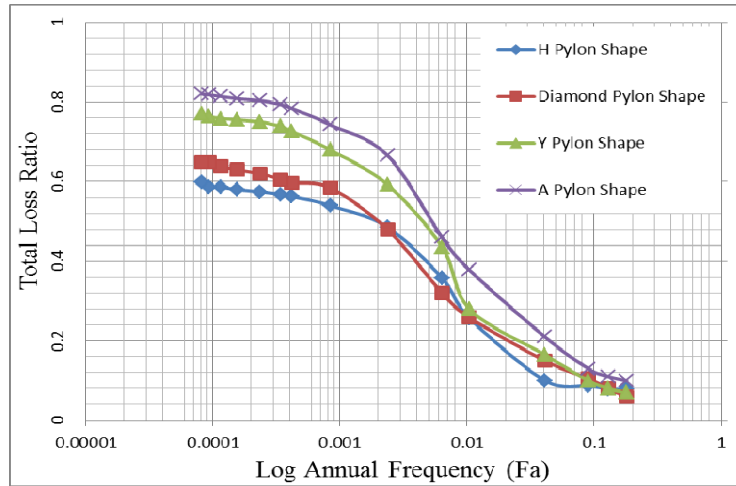


Fig. 14 Total loss ratio curve of the bridge system for the different pylon shapes

shape to achieve a justifiable solution for seismic risk mitigation. Because, up to this part of the discussion only the first criteria (loss) has been considered, it is necessary to consider the construction costs as the second criteria as well, with using proposed process in the following section.

#### 4. Financial-comparative risk assessment using Cost-Loss-Benefit (CLB) method

It should be noted that, although the fragility and loss curves provide a more accurate comparison than seismic responses, they still do not provide perfect judgments. Deciding between different structural schemes can be only justifiable when the construction costs for each scheme are examined alongside its probable loss due to earthquake. So, the financial-comparative seismic risk assessment as a perfect decision-making tool of this paper is developed using the results of section 3.2 and the proposed CLB method. In other words, the perfect choice could be selected between different feasible structural design schemes using the results of this simple method. Hence, decision-making of the optimal pylon shape can be done by considering the construction costs and probable earthquake losses simultaneously. Also, considering the currency value differences in different countries, the advantage of the CLB method is that it uses relative values. Hence, it can be applied to any structure without being affected by the absolute prices.

The Expected Annual Loss (EAL) is calculated based on the method proposed by Solberg *et al.* (2008) using Eqs. (9)-(10)

$$EAL = \bar{x} [0.6 + 0.2(3.5^{b\beta_{lnD}} + 3.5^{-b\beta_{lnD}})] \quad (9)$$

Where  $EAL$  is the Expected Annual Loss as a fraction of structure cost,  $b$  is the constant of the hazard curve in Eq. (8),  $\beta_{lnD}$  is the standard deviation corresponding to the PSDM, and  $\bar{x}$  is the mean variable for the four damage states and is obtained using Eq. (10) (Solberg *et al.* 2008)

$$\tilde{x} = \sum_{i=1}^4 f_{a_i} \Delta LR_i \tag{10}$$

Where  $\Delta LR_i = LR_i - LR_{i-1}$ , and  $f_{a_i}$  is the annual frequency of the occurrence of the PGA for which the probability of exceeding the  $i$ 'th damage state is 50%.

In the CLB method, one of the design schemes must be selected as benchmark and then other schemes can be evaluated relatively. For this purpose, a factor called Benefit Ratio (BR) is calculated for each design scheme, which will be used as a criteria to compare different design schemes. So BR value for the benchmark scheme is assumed equal to 1 and a BR value greater than 1 for a design scheme indicates that the corresponding design scheme is relatively more beneficial than the benchmark design. Benefit Ratio (BR) is calculated as follows:

If the absolute construction cost for  $S$ th structural scheme is  $C_s$ , then its absolute Expected Annual Loss is calculated by Eq. (11)

$$Loss_s = EAL_s * C_s \tag{11}$$

Where,  $Loss_s$  is the absolute expected annual loss of the  $S$ 'th structural scheme,  $EAL_s$  is the relative Expected Annual Loss of the  $S$ 'th structural scheme and  $C_s$  is the absolute construction costs for  $S$ th structural scheme.

So BR can be calculated by Eq. (12) according to its definition as: "total benefit resulted from using an alternative design scheme instead of existing design scheme"

$$BR_s = \left(\frac{C_{s=1}}{C_s}\right) \times \left(\frac{Loss_{s=1}}{Loss_s}\right) \tag{12}$$

Where  $C_{s=1}$  is the absolute construction cost of the existing structure which is selected as the benchmark design scheme, and  $Loss_{s=1}$  is the absolute expected annual loss of the benchmark design scheme.

According to the Eq. (11), Eq. (12) can be simplified to

$$BR_s = \left(\frac{C_{s=1}}{C_s}\right)^2 \times \left(\frac{EAL_{s=1}}{EAL_s}\right) \tag{13}$$

Where  $EAL_{s=1}$  is the relative expected annual loss of the benchmark design scheme.

Hence, by defining a simple BR factor, the double criterion decision-making problem turns into a single criteria decision-making problem where BR is the only decision-making criteria.

Note that in this method the construction costs of the different design schemes should not be evaluated using their absolute values; instead they must be evaluated relative to the benchmark design. To achieve this, we use the "Material Volume Coefficient" from results of the Table 1, and a logical coefficient to consider the conditions of constructing each pylon shape of design scheme. So based on the field researches and the pre-construction studies of the Ahvaz cable-stayed bridge performed by the consulting engineers of the project, construction conditions coefficient for diamond shape, H, A and Y shape are considered 1, 0.76, 0.92 and 0.85 respectively. Also, based on mentioned study for Ahvaz cable-stayed bridge, the construction of pylons takes 23% of the total costs of the bridge with diamond pylon shape which is reported in Table 1 earlier. Finally, the construction costs of quadruple bridge design schemes relative to the benchmark bridge which has a diamond pylon shape, are presented in Table 8 along with the results of the CLB method.

The obtained BR values indicate that even the A and Y shape pylons designed based on seismic guidelines, when evaluated by financial risk assessment, are not appropriate options for the studied

Table 8 The CLB method results and data

Pylon Shape	Material Volume Coefficient	Pylon Constructing Condition Coefficient	$(\frac{C_{s=1}}{C_s})$	$(\frac{EAL_{s=1}}{EAL_s})$	$BR_s$
Diamond Shape	1	1	1	1	1
H Shape	1.06	0.76	0.96	1.14	1.05
Y Shape	1.22	0.92	0.85	0.93	0.67
A Shape	1.13	0.85	0.91	0.72	0.6

span. Although the bridge with H shape pylon has higher primary costs due to its larger dimensions, compared to diamond shape pylon it has a lower loss, and finally higher BR value. Hence, considering simultaneously construction cost and seismic loss, H shape is the optimal option for the studied span of cable-stayed bridge.

## 5. Conclusions

In this paper, a method for the seismic risk assessment process is proposed with a financial-comparative approach with the purpose of decision-making of the optimal pylon shape as an alternative scheme for a constructed cable-stayed bridge. In this process, seismic fragility assessment is done based on the proposed IDA and UD method; And jointly probabilistic model is used to obtain the fragility of the entire bridge system from the fragility of the components. In combination of the loss assessment and fragility assessment, the seismic risk assessment process is developed with a financial-comparative approach using the proposed cost-loss-benefit method. Hence the double criterion decision-making problem of the optimal shape for the pylon is solved by simultaneously analyzing the construction costs and losses due to probable earthquakes. The results of the problem solving process are summarized as follows:

- Ramberg-Osgood relationship properly estimates the mean lognormal distribution of the PSDM of the cable-stayed bridge.
- Elastomeric bearing pad is the most fragile component of the cable-stayed bridge system, except for the H shape pylon case.
- The fragility of pylon head displacement for A shape pylon is higher than its fragility for other pylon shapes.
- About the pylon curvature: H and Y shape pylons have the highest damage probability and diamond shape pylon has the lowest damage probability.
- Cables are more fragile in the A shape pylon than other pylon shapes.
- The elastomeric bearing pad displacement damage index has the lowest exceedance probability in the H shape pylon, and the highest exceedance probability in the diamond shape pylon.
- Generally, the damage probability of the entire bridge system descends in this order: A, Y, diamond, and H shape.
- According to the loss analysis, generally H and diamond shape pylons have low loss ratios, and expected annual loss of the H shape pylon is lower than that of the diamond shape.
- Bridge with the H shape pylon has higher primary cost than bridge with the diamond shape

pylon, but because the H shape has a higher BR value, it is the optimal option for the studied span of the cable-stayed bridge.

### Future works

The damage of elastomeric bearing pad (as the most fragile component of the system) in longitudinal earthquakes, which was the main reason of the H shape pylon superiority, affected the decision-making, severely; Since the H shape resistance against longitudinal earthquakes compensated the weakness of elastomeric bearing pad. Therefore, in case of using a bearing device with more efficiency in seismic performance, further research must be conducted to compare the pylon shapes.

Svensson (2013), based on his experiences, presented recommendations about the pylon shapes depending on the span length of the cable-stayed bridges. Hence, it is needed to re-examine the pylon shapes for spans longer than the studied one in this paper.

### Acknowledgments

In the end, the authors thank Hexa consulting engineers who designed the Ahvaz cable-stayed bridge, which is the benchmark of our study, and Abbas Tahani MSc (Vice-President of the Board, Manager of Design Department) who provided us with the detailed information on the construction cost studies of the Ahvaz cable-stayed bridge project.

### References

- Agrawal, A.K., Ghosn, M., Alampalli, S. and Pan, Y (2012), "Seismic fragility of retrofitted multispan continuous steel bridges in New York", *J. Bridge Eng.*, **17**(4), 562-575.
- Aviram, A., Mackie, K. and Stojadinovic, B. (2008), "Guidelines for nonlinear analysis of bridge structures in California (Technical Report)", Pacific Earthquake Engineering Research Center(PEER), University of California, Berkeley.
- Barnawi, W. and Dyke, S. (2014), "Seismic fragility relationships of a cable-stayed bridge equipped with response modification systems", *J. Bridge Eng.* **19**(SPECIAL ISSUE: Recent Advances in Seismic Design, Analysis, and Protection of Highway Bridges), A4013003.
- Bhagwat, M., Sasmal, S., Novák, B. and Upadhyay, A. (2009), "Dynamic performance evaluation of straight and curved cable-stayed bridges", *Bridge Struct.: Assess., Des. Constr.*, **5**(2-3), 87-95.
- Bhagwat, M., Sasmal, S., Novak, B. and Upadhyay, A. (2011), "Investigations on seismic response of two span cable-stayed bridges", *Earthq. Struct.*, **2**(4), 337-356.
- Caltrans, S.D.C. (2004), *Caltrans Seismic Design Criteria version 1.3*, California Department of Transportation, Sacramento, California.
- Calvi, G.M., Sullivan, T.J. and Villani, A. (2010), "Conceptual seismic design of cable-stayed bridges", *J. Earthq. Eng.*, **14**(8), 1139-1171.
- Casciati, F., Cimellaro, G.P. and Domaneschi, M. (2008), "Seismic reliability of a cable-stayed bridge retrofitted with hysteretic devices", *Comput. Struct.*, **86**(17), 1769-1781.
- Chang, K.C., Mo, Y.L., Chen, C.C., Lai, L.C. and Chou, C.C. (2004), "Lessons learned from the damaged Chi-Lu cable-stayed bridge", *J. Bridge Eng.*, **9**(4), 343-352.
- Decò, A. and Frangopol, D.M. (2011), "Risk assessment of highway bridges under multiple hazards", *J. Risk*

- Res.*, **14**(9), 1057-1089.
- Domaneschi, M. (2010), "Feasible control solutions of the ASCE benchmark cable-stayed bridge", *Struct. Control Health Monit.*, **17**(6), 675-693.
- Domaneschi, M. and Martinelli, L. (2012), "Performance comparison of passive control schemes for the numerically improved ASCE cable-stayed bridge model", *Earthq. Struct.*, **3**(2), 181-201.
- Domaneschi, M. and Martinelli, L. (2013), "Extending the benchmark cable-stayed bridge for transverse response under seismic loading", *J. Bridge Eng.*, **19**(3), 04013003.
- Fang, K.T., Lin, D.K., Winker, P. and Zhang, Y. (2000), "Uniform design: theory and application", *Technometrics*, **42**(3), 237-248.
- Fangfang, G., Youliang, D., Jianyong, S., Wanheng, L. and Aiqun, L. (2014), "Passive control system for seismic protection of a multi-tower cable-stayed bridge", *Earthq. Struct.*, **6**(5), 495-514.
- Farquhar, D.J. (2008), *Cable-stayed bridges. ICE Manual of Bridge Engineering (2<sup>nd</sup> edition)*, Institution of Civil Engineers, London, UK.
- Ferguson, T.S. (1967), *Mathematical Statistics: A Decision Theoretic Approach*, Academic Press, New York, USA.
- Gholipour, Y., Bozorgnia, Y., Rahnamaa, M. and Berberian, M. (2008), "Probabilistic seismic hazard analysis, phase I-Greater Tehran Regions (Technical Report)", College of Engineering, University of Tehran.
- Jara, J.M., Galván, A., Jara, M. and Olmos, B. (2013a), "Procedure for determining the seismic vulnerability of an irregular isolated bridge", *Struct. Infrastruct. Eng.*, **9**(6), 516-528.
- Jara, J.M., Villanueva, D., Jara, M. and Olmos, B.A. (2013b), "Isolation parameters for improving the seismic performance of irregular bridges", *Bull. Earthq. Eng.*, **11**(2), 663-686.
- Jara, J.M., López, M.G., Jara, M. and Olmos, B.A. (2014), "Rotation and damage index demands for RC medium-length span bridges", *Eng. Struct.*, **74**, 205-217.
- Kawashima, K., Unjoh, S. and Tunomoto, M. (1993), "Estimation of damping ratio of cable-stayed bridges for seismic design", *J. Struct. Eng.*, **119**(4), 1015-1031.
- Khan, R.A., Datta, T.K. and Ahmad, S. (2006), "Seismic risk analysis of modified fan type cable stayed bridges", *Eng. Struct.*, **28**(9), 1275-1285.
- Khan, R.A. and Datta, T.K. (2010), "Probabilistic risk assessment of fan type cable-stayed bridges against earthquake forces", *J. Vib. Control*, **16**(6), 779-799.
- Kim, D., Yi, J.H., Seo, H.Y. and Chang, C. (2008), "Earthquake risk assessment of seismically isolated extradosed bridges with lead rubber bearings", *Struct. Eng. Mech.*, **29**(6), 689-707.
- Li, H., Liu, J. and Ou, J. (2009), "Investigation of seismic damage of cable-stayed bridges with different connection configuration", *J. Earthq. Tsunami*, **3**(03), 227-247.
- Mackie, K.R. and Stojadinović, B. (2005), "Fragility basis for California highway overpass bridge seismic decision making (Technical Report)", Pacific Earthquake Engineering Research Center, College of Engineering, University of California, Berkeley.
- Makris, N. and Zhang, J. (2002), "Structural characterization and seismic response analysis of a highway overcrossing equipped with elastomeric bearings and fluid dampers: A case study (Technical Report)", Pacific Earthquake Engineering Research Center, PEER, University of California, Berkeley.
- Mander, J.B., Dhakal, R.P., Mashiko, N. and Solberg, K.M. (2007), "Incremental dynamic analysis applied to seismic financial risk assessment of bridges", *Eng. Struct.*, **29**(10), 2662-2672.
- Mander, J.B., Priestley, M.J.N. and Park, R. (1988), "Theoretical stress-strain model for confined concrete", *J. Struct. Eng.*, **114**(8), 1804-1826.
- Mander, J.B., Sircar, J. and Damnjanovic, I. (2012), "Direct loss model for seismically damaged structures", *Earthq. Eng. Struct. Dyn.*, **41**(3), 571-586.
- Muntasir Billah, A.H.M. and Shahria Alam, M. (2014), "Performance-based prioritisation for seismic retrofitting of reinforced concrete bridge bent", *Struct. Infrastruct. Eng.*, **10**(8), 929-949.
- Nazmy, A.S. and Abdel-Ghaffar, A.M. (1990), "Three-dimensional nonlinear static analysis of cable-stayed bridges", *Comput. Struct.*, **34**(2), 257-271.

- Nielson, B.G. and DesRoches, R. (2007), "Seismic fragility methodology for highway bridges using a component level approach", *Earthq. Eng. Struct. Dyn.*, **36**(6), 823-839.
- Olmos, B.A., Jara, J.M. and Jara, M. (2012), "Influence of some relevant parameters in the seismic vulnerability of RC bridges", *Earthq. Struct.*, **3**(3-4), 365-381.
- Pacific Earthquake Engineering Research Center (PEER). (2008), "Users manual for the PEER ground motion database web application", University of California, Berkeley.
- Padgett, J.E., Dennemann, K. and Ghosh, J. (2010), "Risk-based seismic life-cycle cost-benefit (LCC-B) analysis for bridge retrofit assessment", *Struct. Safety*, **32**(3), 165-173.
- Pang, Y., Wu, X., Shen, G. and Yuan, W. (2013), "Seismic fragility analysis of cable-stayed bridges considering different sources of uncertainties", *J. Bridge Eng.*, **19**(4), 04013015.
- Raheem, S.E.A. and Hayashikawa, T. (2013), "Energy dissipation system for earthquake protection of cable-stayed bridge towers", *Earthq. Struct.*, **5**(6), 657-678.
- Ren, W.X. and Obata, M. (1999), "Elastic-plastic seismic behavior of long span cable-stayed bridges", *J. Bridge Eng.*, **3**(194), 194-203.
- Ross, S.M. (2009), *Introduction to Probability and Statistics for Engineers and Scientists*, Academic Press, New York, USA.
- SAP2000 (2005), "Linear and nonlinear static and dynamic analysis and design of three-dimensional structures: basic analysis reference manual", Computers and Structures Inc., CSI, Berkeley, California.
- Sasmal, S., Ramanjaneyulu, K. and Lakshmanan, N. (2007), "Priority ranking towards condition assessment of existing reinforced concrete bridges", *Struct. Infrastruct. Eng.*, **3**(1), 75-89.
- Seismosoft. (2013), SeismoMatch v2.1-A computer program for spectrum matching of earthquake records, available from <http://www.seismosoft.com>.
- Shah, S.G., Desai, J.A. and Solanki, C.H. (2010), "Effect of pylon shape on seismic response of cable-stayed bridge with soil structure interaction", *Int. J. Civ. Struct. Eng.*, **1**(3), 667-682.
- Shinozuka, M., Kim, S.H., Kushiyama, S. and Yi, J.H. (2002), "Fragility curves of concrete bridges retrofitted by column jacketing", *Earthq. Eng. Eng. Vib.*, **1**(2), 195-205.
- Solberg, K.M., Dhakal, R.P., Mander, J.B. and Bradley, B.A. (2008), "Computational and rapid expected annual loss estimation methodologies for structures", *Earthq. Eng. Struct. Dyn.*, **37** (1), 81-101.
- Svensson, H. (2013), *Cable-Stayed Bridges: 40 Years of Experience Worldwide*, John Wiley & Sons. New York, USA.
- Tang, M.C. (1992), "Guidelines for the design of cable-stayed bridges", American Society of Civil Engineers (ASCE), New York.
- Tesfamariam, S., and Goda, K. (Eds.). (2013), *Handbook of Seismic Risk Analysis and Management of Civil Infrastructure Systems*, Woodhead Publishing Series in Civil and Structural Engineering, Cambridge, UK.
- Vamvatsikos, D. and Cornell, C.A. (2002), "Incremental dynamic analysis", *Earthq. Eng. Struct. Dyn.*, **31**(3), 491-514.
- Yi, J.H., Kim, S.H. and Kushiyama, S. (2007), "PDF interpolation technique for seismic fragility analysis of bridges", *Eng. Struct.*, **29**(7), 1312-1322.
- Wang, B. and Yuan, W. (2009), "Risk- and performance-based seismic analysis for long-span cable-stayed bridges", *TCLÉE 2009: Lifeline Earthquake Engineering in a Multihazard Environment*, Oakland, California, USA, June 28-July 1.